

2-Quinoxalinylnitrenes and 4-Quinazolinylnitrenes: Rearrangement to Cyclic and Acyclic Carbodiimides and Ring-Opening to Nitrile Ylides

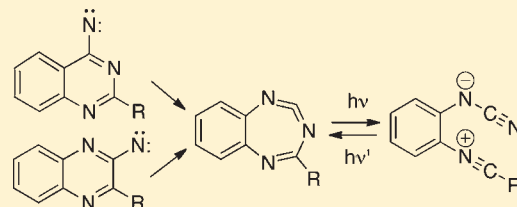
David Kvaskoff, Michael Vosswinkel, and Curt Wentrup*

School of Chemistry and Molecular Biosciences, The University of Queensland, Brisbane, Qld 4072, Australia

Supporting Information

ABSTRACT: This work was undertaken with the aim to obtain direct evidence for the interrelationships between hetarylnitrenes, their ring-expanded cyclic carbodiimide isomers, and ring-opened nitrile ylides. Tetrazolo[1,5-*a*]quinoxaline **11T** and tetrazolo[5,1-*c*]quinazoline **13T** undergo valence tautomerization to the corresponding azides **11A** and **13A** on mild flash vacuum thermolysis (FVT). Photolysis in Ar matrixes at ca. 15 K affords the triplet nitrenes **12** and **14**, identified by ESR, UV, and IR spectroscopy. The nitrenes are converted photochemically to the seven-membered ring carbodiimide **15** followed by the open-chain carbodiimide **22**.

The 3-methoxy- and 3-chloro-2-quinoxalinylnitrenes **24** yield the ring-expanded carbodiimides **26** very cleanly on matrix photolysis, whereas FVT affords *N*-cyanobenzimidazoles **28**. The ring-opened nitrile ylides **36** and **49** are identified as intermediates in the photolyses of 2-phenyl-4-quinazolinylnitrene **32** and 7-nitro-2-phenyl-4-quinazolinylnitrene **47**. In these systems, a photochemically reversible interconversion of the seven-membered ring carbodiimides **35** and **48** and the nitrile ylides **36** and **49** is established. Recyclization of open-chain nitrile ylides is identified as an important mechanism of formation of ring contraction products (*N*-cyanobenzimidazoles).

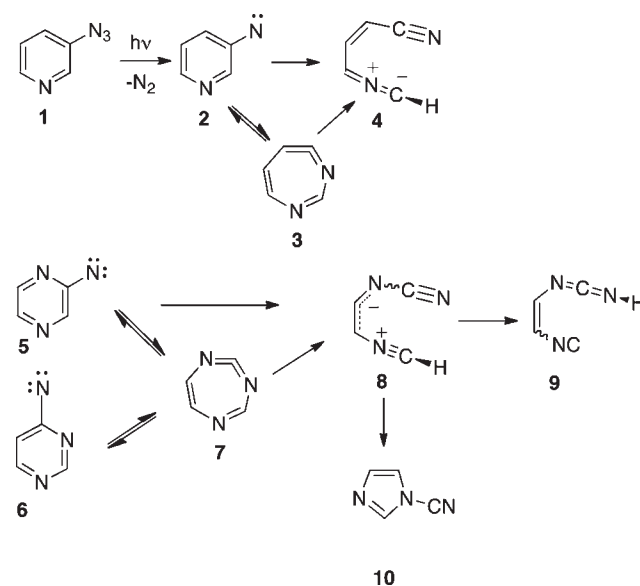


INTRODUCTION

Nitrenes can undergo bewildering rearrangements involving several consecutive reactive intermediates. It is the purpose of this work to identify each of these intermediates accurately and determine their interrelationships. Thus, for example, photolysis of 3-pyridyl azide **1** in low-temperature Ar matrixes leads to ring opening of the nitrene **2** to the nitrile ylide **4**, which was directly observed by IR and UV spectroscopy.¹ However, the ring-expanded cyclic ketenimine **3** was not observed. Ring expansion to seven-membered ring ketenimines and carbodiimides is the normal fate of aryl- and hetarylnitrenes under both photochemical and thermal conditions,² so the failure to detect **3** is worrisome. Ring opening of 3-quinolylnitrene to the corresponding nitrile ylide has been documented, but again the expected cyclic ketenimine was either not observable, or observable only by a very weak peak at 1910 cm⁻¹ in the matrix IR spectrum.³

Interconversion of 2-pyrazinylnitrenes **5** and 4-pyrimidinylnitrenes **6** was demonstrated by ¹⁵N-labeling and postulated to take place via the triazacycloheptatetraenes **7**. A very weak peak at 1973 cm⁻¹ appearing in the IR spectra during the first few minutes of Ar matrix photolysis of the unsubstituted tetrazole precursors was tentatively ascribed to **7**, but this absorption disappeared rapidly, as the end products isocyanovinylcarbodiimide **9** and 1-cyanoimidazole **10** were formed (Scheme 1). Calculations at the G3(MP2) and CASPT2/6-31G* levels supported a facile and exothermic ring opening of **7** to the nitrile ylide **8** via a barrier of ca. 4 kcal/mol, but the ylide was not observed.⁴ No system has yet been reported where the nitrene,

Scheme 1. Reactions of Nitrenes via Ring-Opened Nitrile Ylides 4 and 8



the ylide, and the seven-membered ring cumulene could all be observed and interchanged.

Received: December 11, 2010

Published: March 18, 2011

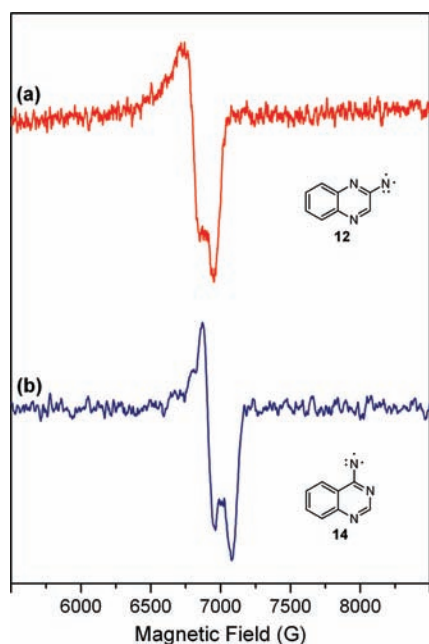


Figure 1. Quinoxalinylnitrenes and Quinazolinylnitrenes. (a) Photolysis of tetrazoloquinoxaline **11T**/2-azidoquinoxaline **11A** at 308 nm for 2 min. 2-Quinoxalinylnitrene **12**: $X_2 = 6820$ G, $Y_2 = 6965$ G, $H_0 = 3468.3$ G, $\nu = 9.720$ GHz G; $D/hc = 0.9538 \pm 0.0025$, $E/hc = 0.0030 \pm 0.0001$ cm⁻¹ (average of three experiments). (b) Photolysis of tetrazoloquinazoline **13T**/4-azidoquinazoline **13A** at 308 nm for 5 min. 2-Quinazolinylnitrene **14**: $H_0 = 3468.3$ G, 6911 G, $Y_2 = 7077$ G, $H_0 = G$, $\nu = 9.720$ GHz, $X_2 = 6911$, $Y_2 = 7077$ G, $\Delta m_s = 2$: 1550 G; $D/hc = 0.9934 \pm 0.0016$, $E/hc = 0.0034 \pm 0.0001$ cm⁻¹ (average of three experiments).

We have now investigated the benzo derivatives **11**, **13**, **24**, **31**, and **46**, where conclusive direct evidence for the nitrenes **12**, **14**, **32**, and **47**, the 7-membered ring intermediates **15**, **26**, **35**, and **48**, and the nitrile ylides **36** and **49** has been obtained.

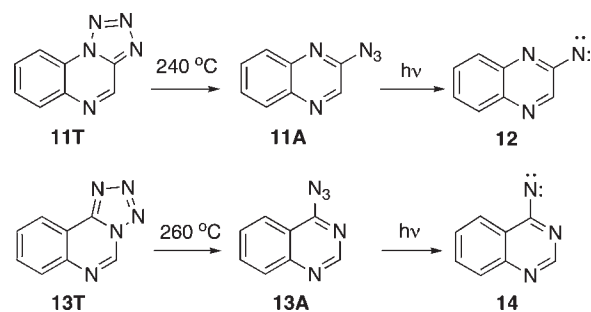
RESULTS AND DISCUSSION

2-Quinoxalinylnitrenes and 4-Quinazolinylnitrenes: ESR. Mild flash vacuum thermolysis (FVT) of the isomeric tetrazoles **11T** and **13T** at 200–300 °C, that is, below the temperature of decomposition with N₂ loss, results in partial ring opening to the azides **11A** and **13A**, which can be isolated in Ar matrices at ca. 15 K. Azide **11A** gives rise to strong IR absorptions at 2157, 2127, and 1308 cm⁻¹, and azide **13A** at 2180, 2140, and 1363 cm⁻¹ (see Figures S1 and S2, Supporting Information).

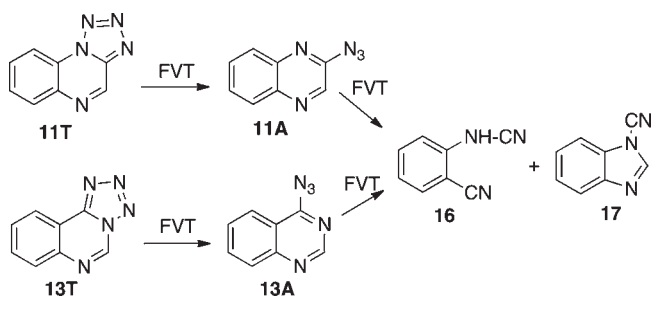
Photolysis of the matrix-isolated tetrazole/azide mixtures **11T/11A** and **13T/13A** for 2–5 min ($\lambda = 308$ nm) at ca. 15 K resulted in ESR spectra typical of triplet heteroaromatic nitrenes (Scheme 2, Figure 1) and assigned to **12** and **14**, respectively.

The ESR spectra of the two nitrenes were corroborated by simulations using the Xsophe software⁵ (Figure S3, Supporting Information). Moreover, the D values are in excellent agreement with expectations based on a correlation between calculated natural electron spin densities with experimental D values.⁶ Nitrenes **12** and **14** were long-lived on irradiation at 308 nm but disappeared at $\lambda > 515$ and 640 nm, respectively (Figures S4 and S5, Supporting Information). In agreement with these observations, the nitrenes show pronounced absorptions in the visible region of the spectrum (Figure 2).

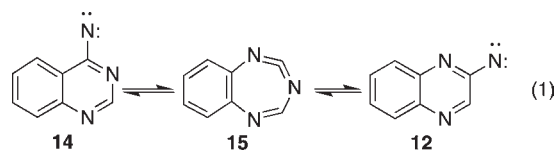
Scheme 2. Nitrenes Generated by Matrix Photolysis and Observed by ESR



Scheme 3. FVT Products



Preparative FVT. Preparative FVT of either **11** or **13** at 450–600 °C afforded two products **16** and **17** in nearly quantitative yield (ratio ca. 55:45)⁷ (Scheme 3 and Figures S1, S2 and S6). The 7-membered triazacycloheptatetraene **15**, the expected link between the two nitrenes (eq 1), was not observable under these conditions. It was, however, formed on matrix photolysis.



Matrix Photolysis: IR and UV. The Ar matrix photolyses of the azides **11A** and **13A** were monitored by UV and IR spectroscopy. Deposition of tetrazole **11T** through the FVT tube at 200–300 °C generated a matrix containing the tetrazole together with a small amount of the azide **11A** (cf. Figures S1 and S2, Supporting Information). Similar deposition of tetrazole **13T** afforded a matrix containing a substantial amount of azide **13A**. Photolysis of these azides **11A** and **13A** at $\lambda = 308$ nm afforded the UV-visible spectra shown in Figures 2 and S7. Although the two spectra are surprisingly different, they are in good agreement with calculations for the triplet states of nitrenes **12** and **14** at the TD-UB3LYP/6-31G** and BPW91/6-31G** levels (Figure S7). The visible spectrum of 4-quinazolinylnitrene **14** is similar to that of 2-quinazolinylnitrene published previously,⁷ the structured absorptions being due in part to vibrational progressions. Irradiation in the long wavelength visible absorption bands causes disappearance of the ESR spectra (Figures S4 and S5). Absorptions up to 650 nm are also observed for the 3-chloro- and 3-methoxy-2-quinoxalinylnitrenes **25b** and **25a** (Figures 7 and S13, respectively). Weak absorptions up to ca. 600 nm have been

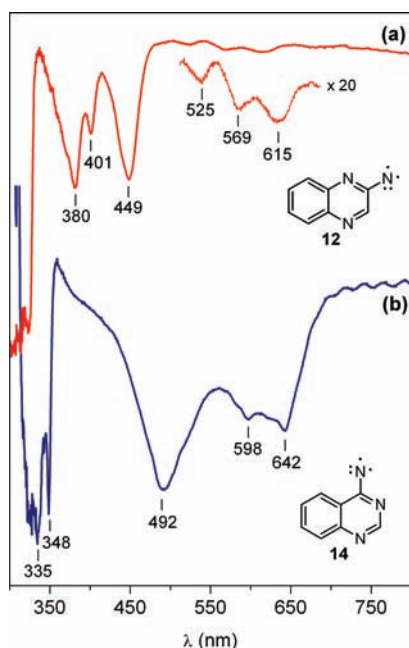


Figure 2. UV–vis difference spectra. (a) Photolysis of 2-azidoquinoxaline **11A** at 308 nm for 9 min (not shown), followed by photolysis at $\lambda > 395$ nm for 2 min. (b) Photolysis of 4-azidoquinazoline **13A** at 308 nm for 10 min (not shown), followed by photolysis >610 nm for 20 min. Negative bands are assigned to the disappearing nitrenes **12** and **14**, respectively. Ordinate in arbitrary absorbance units. See Figure S7 for calculated UV–vis spectra.

observed for the naphthylnitrenes^{2b} and 3-quinolylnitrene.³ It should be noted that there are still large amounts of the unchanged tetrazoles (**11T** and **13T**, respectively), which do not appear in the difference spectra presented in Figure 2.

The irradiation of the matrix containing 4-quinazolinyl nitrene **14** (having the UV–vis spectrum of Figure 2b) with visible light ($\lambda > 610$ nm) afforded a new product with a strong absorption at 2005 cm^{-1} in the IR spectrum, which is ascribed to the cyclic carbodiimide **15** due to excellent agreement with the calculated spectrum (Figure 3). The intensities of the IR (Figure 3) and UV spectra assigned to the triplet nitrene **14** decreased at the same time. Formation of **15** and disappearance of **14** was also observed on photolysis of the matrix at $\lambda > 475$ nm or at $\lambda = 435\text{--}520$ nm for 2 min. In the latter case, substantial amounts of the ring-opened carbodiimide **22** were also formed due to secondary photolysis of **15** (see below).

The cyclic carbodiimide **15** (2005 cm^{-1}) was also obtained by photolysis of the matrix containing 2-quinoxalyl nitrene **12** at $\lambda > 395$ nm (Figure 4), but in this case, a substantial amount of the ring-opened carbodiimide **22** was formed as well (3416 , 2157 , 2131 cm^{-1} ; Figure 4). Nevertheless, compound **15** can be obtained almost pure also in this case by photolysis of a matrix containing a mixture of **11T** and **11A** at $\lambda > 310$ nm (Figure S8). The azide photolyzes much faster than the tetrazole; therefore, much unchanged tetrazole is still present in the final spectra.

Thus, photolysis at the wavelength of the visible absorption of **14** (>610 nm) resulted in the clean disappearance of the absorptions ascribed to nitrene **14** in the ESR (Figure S5), in the UV–vis (Figure 2b) and in the IR spectrum (Figure 3), concomitant with the formation of the cyclic carbodiimide **15**. All

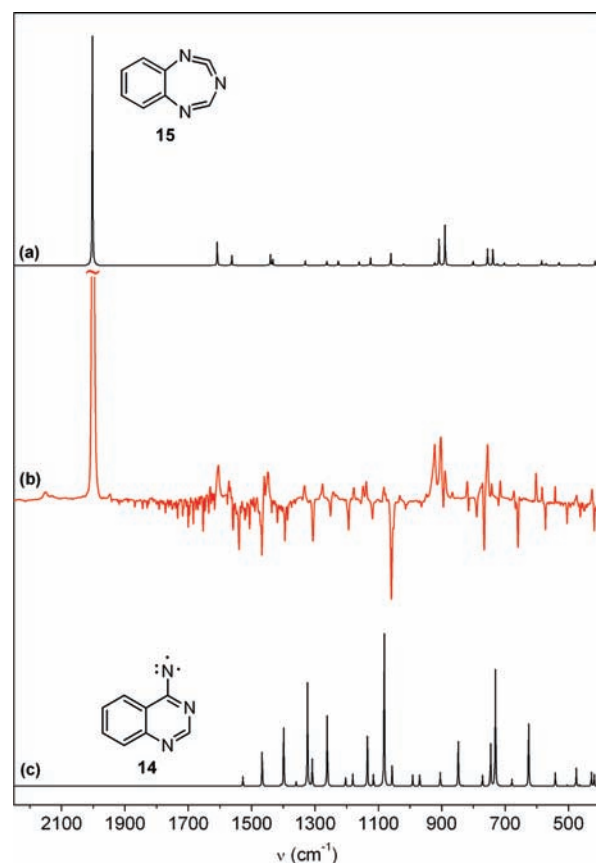


Figure 3. (a) Calculated IR spectrum of cyclic carbodiimide **15** (the strongest absorption at 2005 cm^{-1} is attenuated by a factor of 0.65). (b) Photolysis of 4-azidoquinazoline **13A** at 308 nm for 20 min to generate nitrene **14** (not shown), followed by photolysis at $\lambda > 610$ nm (cutoff filter) for 20 min (positive peaks: **15**, negative peaks: 4-quinazolinyl nitrene **14**). The matrix is the same as the one used for Figure 2b. (c) Calculated IR spectrum of triplet nitrene **14** (B3LYP/6-31G**); wavenumbers scaled by a factor 0.9613). Ordinate in arbitrary absorbance units.

the bands of **14** in the UV–vis spectrum decreased at the same rate (323 , 334 , 348 , 492 , 596 , 621 , 642 nm). In the photolyses of both **11** and **13**, the intensities of the peaks due to the cyclic carbodiimide **15** decreased and eventually disappeared completely upon subsequent broadband UV photolysis to be replaced by the final product, viz. the open-chain carbodiimide **22** (Scheme 4 and Figures 4 and 5; see also Figures S8–S11, Supporting Information). Small amounts of 1-cyanobenzimidazole **17** (2258 cm^{-1}) were also formed in these photolyses. Kinetic monitoring of the broadband photolysis demonstrated that the final, ring-opened product (**22**; 2131 , 2157 , and 3423 cm^{-1}) was formed at the same rate as the disappearance of the 2005 cm^{-1} species **15** (Figure S10).

Several other candidates for the intermediate formed by photolysis of the nitrenes were considered (**18–20**, Chart 1), and their IR spectra were calculated, but none of them matched the experimental spectra.

The experimental spectrum of the open-chain carbodiimide **22** agrees well with a composite of the two calculated conformers *s-Z-22* and *s-E-22* featuring the two main carbodiimide stretching vibrations around $2162\text{--}2157\text{ cm}^{-1}$ and two main isocyanide stretches around 2138 and 2131 cm^{-1} (Figure 5; see

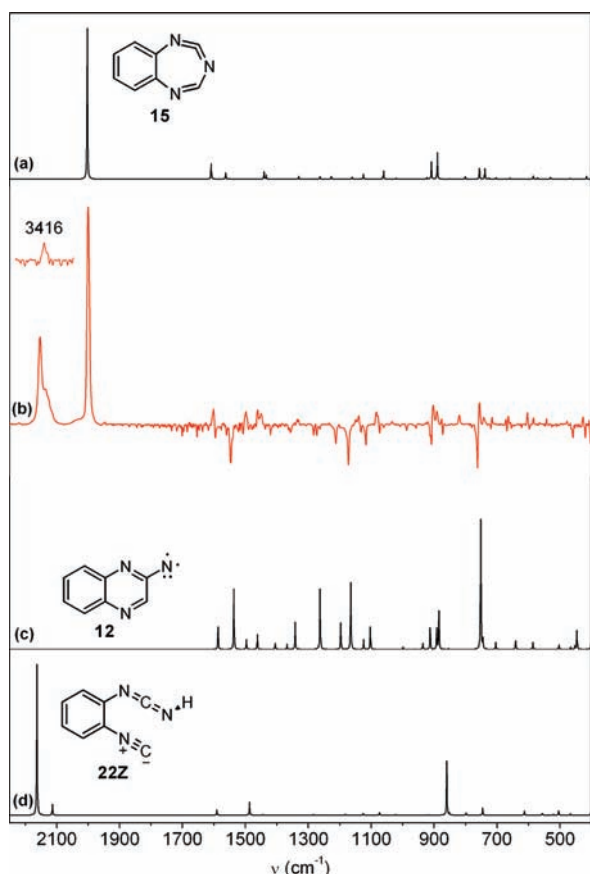
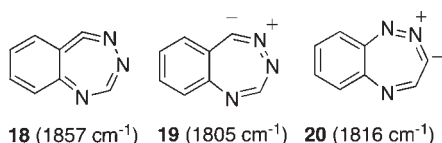


Figure 4. (a) Calculated IR spectrum of cyclic carbodiimide **15** (the strongest absorption at 2005 cm^{-1} is attenuated by a factor of 0.86). (b) Photolysis of 2-azidoquinoxaline **11A** at 308 nm for 9 min to generate 2-quinoxalinylnitrene **12** (not shown), followed by photolysis at $\lambda > 395\text{ nm}$ (cutoff filter) for 2 min (negative bands: nitrene **12**; positive bands: cyclic carbodiimide **15** (2005 cm^{-1} , etc.) and acyclic carbodiimide **22** ($3416, 2157, 2131\text{ cm}^{-1}$)). (c) Calculated IR spectrum of *s*-Z-**22** (see also Figure 5). Calculations at the B3LYP/6-31G** level (wavenumbers scaled by a factor 0.9613). Ordinate in arbitrary absorbance units.

Chart 1. Unobserved Alternatives to Compound **15**^a

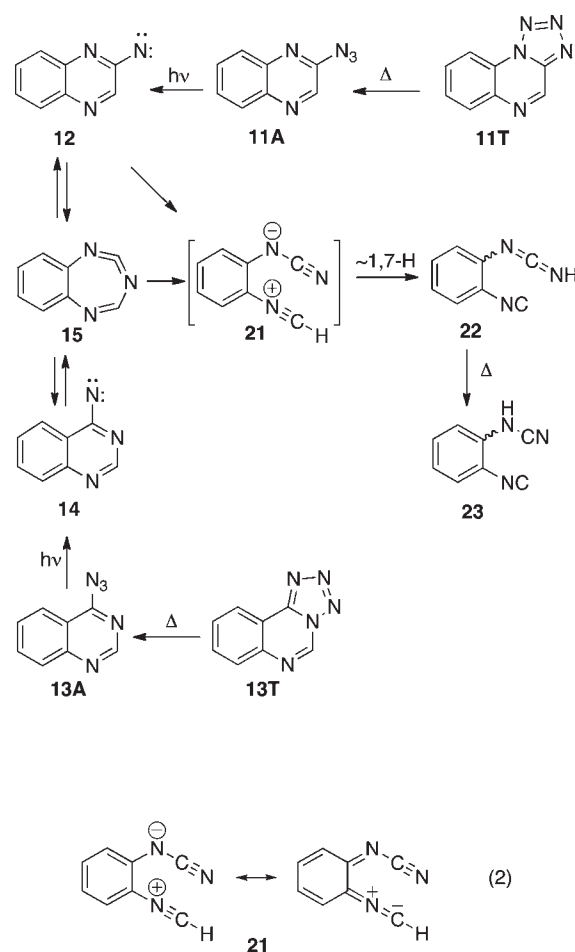


^aMain IR absorptions in cm^{-1} calculated at the B3LYP/6-31+G* level and scaled by a factor 0.9613. Computational details for these as well as the corresponding valence-isomeric triazacycloheptatrienyliidene structures are presented in the Supporting Information.

also Figure S11 for details of the absorptions at 2131 and 2157 cm^{-1}). The structure of **22** was further supported by slow warm-up of the matrix to 40 K, thus, allowing the Ar to evaporate. Further warming to 90 K caused tautomerization to the isocyanophenylcyanamide **23** ($2122, 2145\text{ cm}^{-1}$ (NC); 2253 cm^{-1} (NH-CN); 3300 cm^{-1} (broad, NH)), which was identified by comparison with the calculated spectra of the *s*-Z and *s*-E conformers (Figure S12).

The kinetic experiments (Figure S10) indicate very strongly that compounds **15** and **22** are formed in consecutive reactions.

Scheme 4. Matrix Photolysis Yielding **15** and **22** and Warm-Up Yielding **23**



They do not exclude the possibility that the cyclic carbodiimide **15** reverts to 2-quinoxalinylnitrene **12**, which then undergoes ring opening (cf. Scheme 4). The fact that **22** is already formed on photolysis of nitrene **12** (Figures 4 and S7), but not on similar photolysis of nitrene **14** (Figure 3) indicates that nitrene **12** may, in fact, undergo ring opening to **21** and thence **22**. This is supported by calculations at the B3LYP/6-31G** level, which indicate that the triplet nitrene **12** can ring-open to triplet ylide **21** with an activation barrier of 33 kcal/mol (Scheme 5). In contrast, the ring expansion $12 \rightarrow 15$ requires an activation energy of 46 kcal/mol on the triplet surface. Thus, it is possible that ring expansion is the favored process on the singlet surface, but ring-opening of nitrene **12** to ylide **21** may compete on the triplet surface. The energies of open-shell singlet nitrenes (S_1) have been corrected by using Cramer's method.⁸ Both nitrene ring expansions, $12 \rightarrow 15$ and $14 \rightarrow 15$, are very facile processes on the singlet energy surface with activation barriers of the order of 8–10 kcal/mol (Scheme 5). These computed transition states have some triplet contamination but are still ca. 90% singlet in character. The spin contamination will cause an underestimation of the energies of these transition states. However, the activation energies computed for the naphthyl nitrenes,^{2d} 2-biphenylnitrenes⁹ and 2-pyridylnitrene¹⁰ using the UB3LYP functional were in reasonable agreement with those at CASPT2 levels. The quinoxalinylnitrene **14** can in principle cyclize in two directions, to

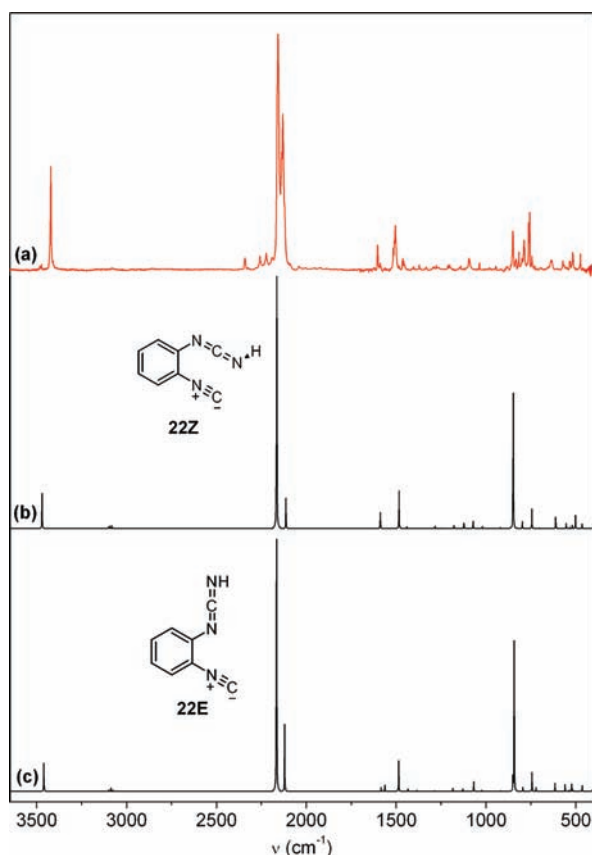
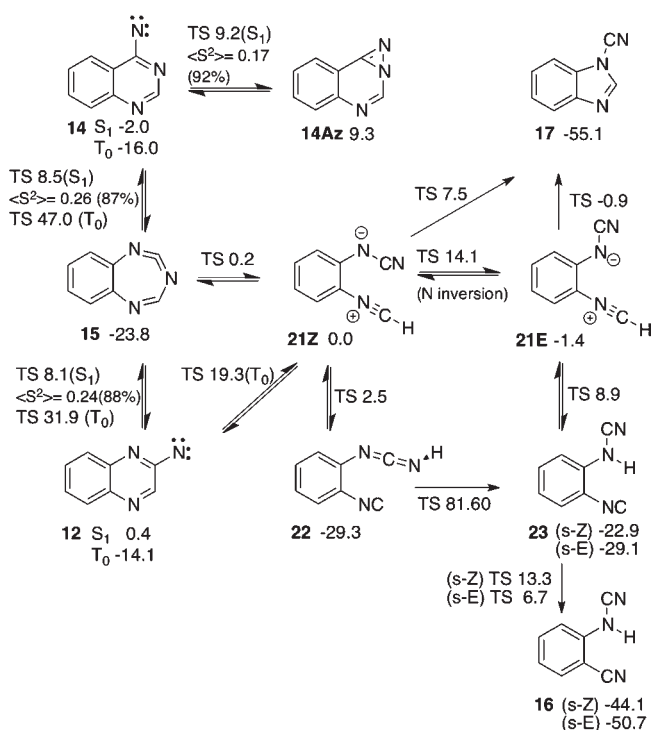


Figure 5. Final photolysis product: acyclic carbodiimide **22**. (a) Spectrum after 878 min of broadband photolysis of Ar matrix isolated tetrazolo[1,5-*a*]quinoxaline **11** at 15 K (selected wavenumbers: 3423, 2157, 2131, 1505, 851, 788, 757, 640, 517, 475, 411 cm^{-1}). (b) Calculated spectrum of acyclic carbodiimide *s*-Z-**22** (3446, 2150, 2112, 1482, 833, 744, 470, 408 cm^{-1}). (c) Calculated spectrum of acyclic *s*-E-**22** (3438, 2151, 2119, 1485, 824, 743, 467, 395 cm^{-1} (all calculations at B3LYP/6-31+G** level, wavenumbers scaled by 0.9613). Ordinate in arbitrary absorbance units. The same compound (**22**) is obtained by photolysis of the cyclic carbodiimide **15** originating from tetrazoloquinazoline **13** (see Figure S9).

give either the diazirine **14Az** (Scheme 5) or the transition state leading to **15**. The two processes have similar activation barriers on the singlet energy surface, but the formation of **15** dominates the subsequent chemistry because **15** is a relatively stable molecule. The ring-opening of **15** to the nitrile ylide **21** has a calculated barrier of ca. 24 kcal/mol (Scheme 5), and the reversion of the ylide **21** to the seven-membered ring **15** is almost barrier-free. The two geometric isomers of **21** can interconvert via a low 14 kcal/mol barrier, and the *E*-isomer **21E** cyclizes to 1-cyanobenzimidazole in an almost barrier-free process (Scheme 5). The *Z*-isomer **21Z** can form the same product via a 7.5 kcal/mol barrier. The 1,7-H shift^{1,3,4} converting **21Z** to the final ring-opened carbodiimide **22** also has a very low barrier (2.5 kcal/mol; Scheme 5). To summarize, the reactions **12** and **14** → **15** → [**21**] → **22** are calculated to be very facile processes, and they correspond to the experimentally observed processes, whereby ylide **21** is still unobserved, and the very low activation barrier for its reversion to **15** will make it extremely difficult to detect. Nevertheless, direct evidence for substituted derivatives of **21** will be given below.

Scheme 5. Calculated Energies of Ground and Transition States (in kcal/mol) at the B3LYP/6-31G** + ZPVE Level



We propose that essentially the same mechanism is followed in the FVT reactions (Schemes 3 and 5). Here, there will be plenty of energy available to form *N*-cyanobenzimidazole **17** by the reaction **21** → **17**, and *o*-cyanamidobenzonitrile **16** by the reactions **21E** → **23** → **26** and **21Z** → **22** → **23**, whereby the last step will be a solid- or liquid-phase tautomerization rather than a 'forbidden' 1,3-H shift with a high calculated barrier (82 kcal/mol) (Scheme 5).

Substituted Quinoxalinylnitrenes and Quinazolinylnitrenes. The methoxy- and chlorotetrazoloquinoxalines **24T** underwent similar matrix photolysis via the azides and nitrenes to afford the cyclic carbodiimides **26** (**26a**: 2000 cm^{-1} ; **26b**: 2005 cm^{-1}) (Scheme 6). Thus, matrix deposition of the 5-methoxytetrazoloquinoxaline **24Ta** through an FVT oven at ca. 250 °C affords a mixture of **24Ta** and the azide **24Aa**. Photolysis of the azide at 308 nm generated the nitrene **25a**, characterized by its IR spectrum (Figure 6), and the UV–vis spectrum which features a red shift of 32 nm compared to **12** (449 nm band → 481 nm; Figure S13). Photolysis in the visible absorption band of **25a** caused disappearance of the nitrene and formation of the seven-membered ring carbodiimide **26a**. The experimental spectra of both the nitrene and the carbodiimide show excellent agreement with the calculated spectra (Figure 6).

Mild FVT of the chloro derivative **24Tb** at 240 °C afforded the corresponding azide **24Ab** (2141, 2137, 1333, and 1330 cm^{-1}). Ar matrix photolysis of the azide at 308 nm led rapidly and cleanly to the nitrene, absorbing up to 650 nm in the UV–visible (Figure 7). The nitrene was observed simultaneously in the IR (Figure 8 and Figure S14). Further photolysis at $\lambda > 610$ nm or at 395–460 nm caused disappearance of the nitrene and clean formation of the cyclic carbodiimide **26b**, whose IR spectrum is again in excellent agreement with calculations (Figure 8; Scheme 6).

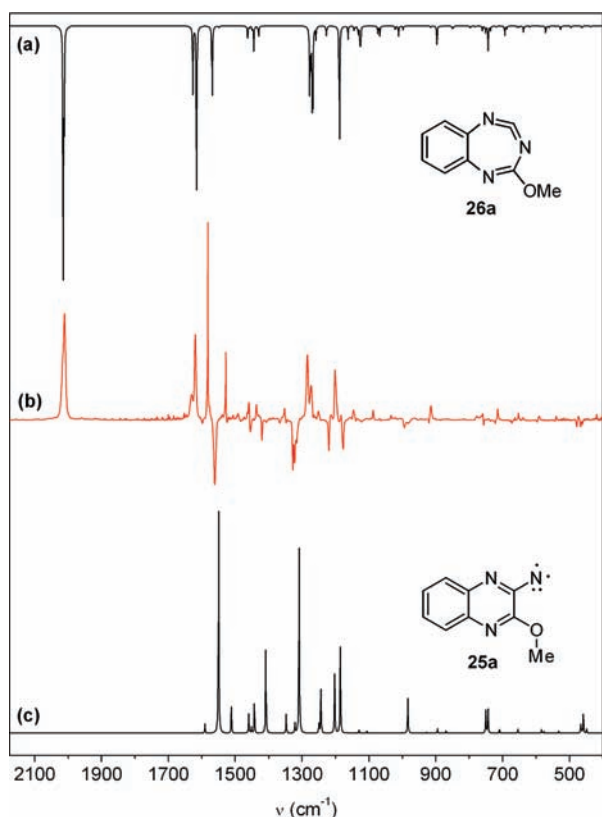
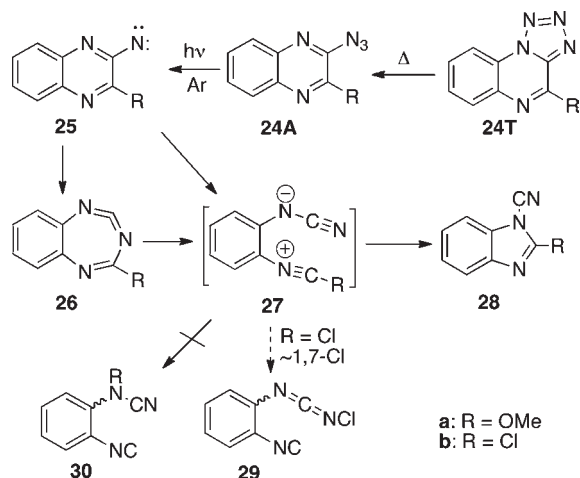


Figure 6. (a) IR spectrum of cyclic carbodiimide **26a** calculated for a 3:1 mixture of the *s-Z* and *s-E* conformers; the calculated energy differences between these two conformers is 3.5 kcal/mol in favor of the *s-Z* conformer. (b) Ar matrix photolysis of 2-azido-3-methoxyquinoxaline **24Aa** at 308 nm for 9 min (generating 3-methoxy-2-quinoxalinylnitrene **25a** (not shown; cf. UV spectrum in Figure S13) followed by photolysis at $\lambda > 434$ nm (cutoff filter) for 2 min. Positive bands, carbodiimide **26a**; negative bands, nitrene **25a**. (c) Calculated IR spectrum of nitrene **25a** (B3LYP/6-31G**); wavenumbers scaled by a factor 0.9613). Ordinates in arbitrary absorbance units.

Scheme 6. Reactions of Substituted Quinoxalinylnitrenes



The photolysis of tetrazoles is usually much slower than that of azides. In the case of **24Tb**, matrix photolysis at 222 nm for 2 min did, however, generate a strong IR spectrum of **26b**, identical to

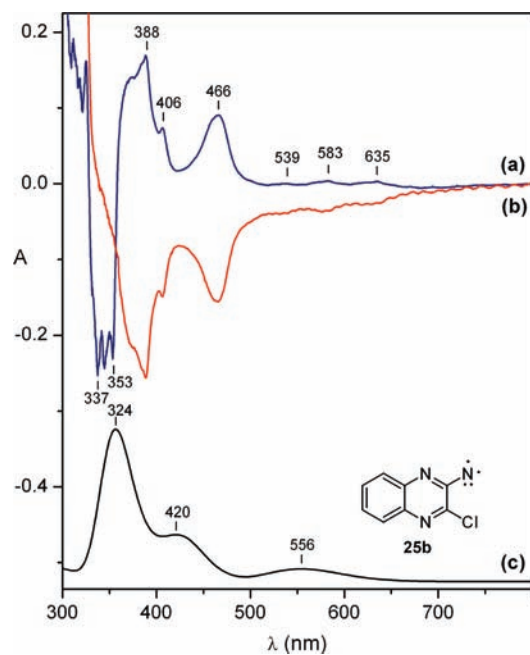


Figure 7. (a) UV-vis difference spectrum from the photolysis of the 2-azido-3-chloroquinoxaline **24Ab** (negative bands 337–353 nm) at 308 nm for 90 s, showing appearance of the nitrene (positive bands). (b) Difference spectrum from photobleaching the nitrene at 395–460 nm for 16 min (photolysis >640 nm results in an analogous but weaker spectrum). (c) Calculated spectrum by TD-B3LYP/6-31+G** convoluted using the SWizard program.¹¹

the one presented in Figure 8. The higher energy available in the 222 nm photolyses caused further rearrangements, particularly the development of new bands at 2266–2262, 2124, and 2078 cm⁻¹ (Figures S15 and S16, Supporting Information). The 2266–2262 cm⁻¹ double band is assigned to the 2-chloro-1-cyanobenzimidazole **28b** (Scheme 6) by comparison with the identical band of **28b** formed and isolated in the FVT reaction of **24Tb** described below. The bands at 2124 and 2078 cm⁻¹ may be due to a 1,7-Cl shift to form the open-chain *N*-chlorocarbodiimide **29** (calculated main bands at 2107 and 2074 cm⁻¹). The 1,7-Cl shift has a calculated barrier of 34 kcal/mol (**27b** → **29**). The potential 1,5-Cl shift to **30** has a calculated barrier of 44 kcal/mol and is not observed. The cyclization of **27** to 2-chloro-1-cyanobenzimidazole **28b** has a calculated barrier of only 9.6 kcal/mol. The cyclic carbodiimide **26b** is calculated to lie 29 kcal/mol below the nitrile ylide **27b**. Additional, weak IR bands at 2156 and 1994 cm⁻¹ and UV-vis absorptions at 370–500 nm (Figure S15) are possibly due to the nitrile ylide **27b** but too weak for a definitive identification. In summary, the cyclic carbodiimides **26** are protected by relatively high energy barriers from further rearrangement in low temperature matrixes, but under FVT conditions, 1-cyanobenzimidazoles **28** can form via readily accessible transition states.

FVT of **24Tb** at temperatures of 450–550 °C caused formation of 2-chloro-1-cyanobenzimidazole **28b**, which was isolated in 47% yield from preparative FVT at 550 °C. In analogy with the reactions described in Schemes 1 and 5 above, it is postulated that ring contraction takes place via ring opening to the unobserved nitrile ylide **27b** (Scheme 6).

The Nitrile Ylides. So far, the nitrile ylides (**21**, **27**) have been elusive. The rapid 1,7-H shifts in the formonitrile ylides **21** makes

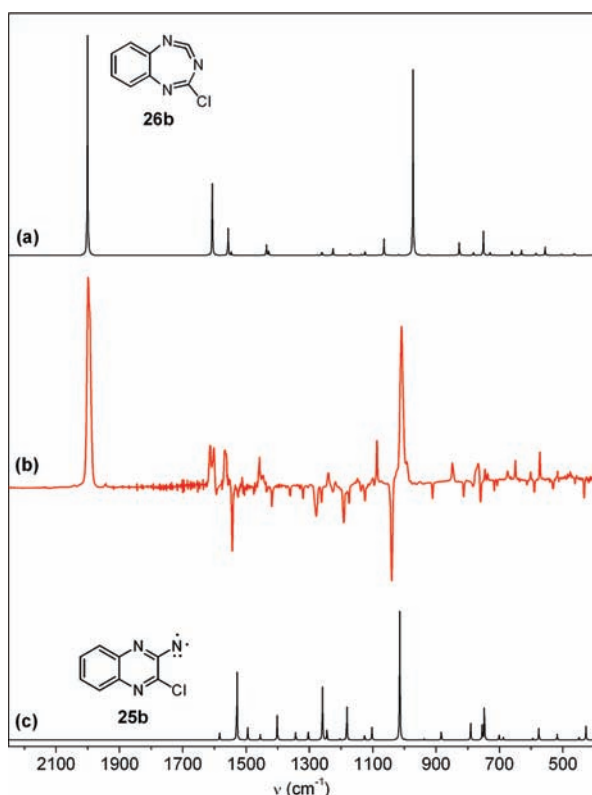
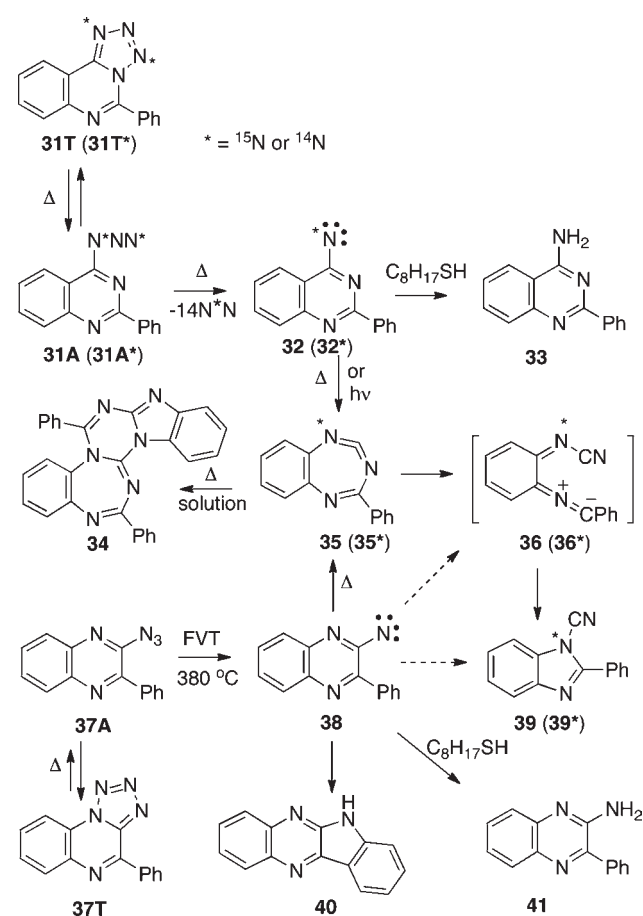


Figure 8. (a) Calculated IR spectrum of 4-chlorotriazabenzocycloheptatetraene **26b** (^{15}Cl isotopomer; wavenumbers scaled by 0.9613). (b) Experimental difference IR spectrum, obtained after 16 min photolysis of 3-chloro-2-quinoxalynitrene **25b** at 395–460 nm in Ar matrix at 15 K. (c) Calculated IR spectrum of nitrene **25b**. All calculations at the B3LYP/6-31G** level. Ordinates in arbitrary absorbance units.

their direct observation difficult. The substituted nitrile ylides **27** cannot undergo the 1,7-H shifts easily, but they can still cyclize rapidly to either **26** or **28** via low activation barriers. Introduction of a phenyl group on the ylidic function makes these species longer-lived and makes it possible to selectively form and destroy them and thus to assign their spectra.

The results of previous investigations¹² of 5-phenyltetrazolo[1,5-*a*]quinazoline/4-azido-2-phenylquinazoline **31T/31A** and the corresponding quinoxalines are summarized in Scheme 7. The 1-cyano-2-phenylbenzimidazole **39** is formed in virtually quantitative yield on FVT of tetrazolo/azidoquinazoline **31T/31A**. The corresponding quinoxaline **37T/37A** affords the same product, but in addition, an 8% yield of the indenoquinoxaline **40** was obtained. The latter product is readily understood as a nitrene cyclization product analogous to the formation of carbazole from 2-biphenylnitrene.^{9,13} Importantly, FVT of **31** did not give rise to **40**. Both nitrenes **32** and **38** underwent H-abstraction in solution in the presence of octanethiol, thereby forming the amines **33** and **41**. Both nitrenes underwent ring contraction to **39** also in solution (thermolysis in benzene in a sealed tube at 180 °C), and a rearranged dimer **34** of the carbodiimide **35** was isolated in both cases. The carbodiimide **35** was observed by IR spectroscopy in the matrix photolysis of **31**. The ^{15}N -labeled tetrazole **31T*** afforded the exclusively ring-labeled cyanobenzimidazole **39*** on FVT. Thus, the most likely course of events is formation of the cyclic carbodiimide **35** from both precursors, ring opening to the as yet unobserved nitrile

Scheme 7. Reactions of Phenyl-Substituted Quinazoliny- and Quinoxalynitrenes



ylide **36**, and recyclization of the latter to form the benzimidazole **39** (Scheme 7). We have now achieved the direct observation of the ylide **36**.

Deposition of the 5-phenyltetrazolo[1,5-*a*]quinazoline **31T** (Schemes 7 and 8) through the FVT oven at 250 °C together with Ar afforded a matrix of the azide **31A** (Figure S17). Photolysis of the azide at $\lambda = 308$ nm generated the nitrene **32** as seen in the ESR spectrum (Figure S18; $D/hc = 0.9992 \pm 0.0014$, $E/hc = 0.0035 \pm 0.0001$ cm⁻¹). However, the IR spectrum obtained under the same conditions revealed a mixture of three products (Figure S17), interpreted as the nitrene **32**, the cyclic carbodiimide **35**, and the ylide **36** due to the observations described below. Irradiation of this matrix with visible light ($\lambda > 610$ nm) caused the disappearance of the nitrene in the ESR spectrum (Figure S18) and in the UV–vis difference spectrum (Figure 9, red curve, $\lambda_{\text{max}} = 735$ and 548 nm; see also Figure S19). The IR difference spectrum of the same matrix showed formation of the cyclic carbodiimide **35**, which absorbs strongly at 2008 cm⁻¹, concomitant with the disappearance of the nitrene (Figure 10). The UV–vis and IR data are in excellent agreement with the calculated spectra (Figures 9 and 10).

Further photolysis of the same matrix at 395 nm (i.e., after photolysis at $\lambda = 308$ nm and $\lambda > 610$ nm) caused disappearance of a species with $\lambda_{\text{max}} = 535$ nm in the UV–vis difference spectrum (Figure 9). This absorption is assigned to ylide **36** because of good agreement with the calculated spectrum

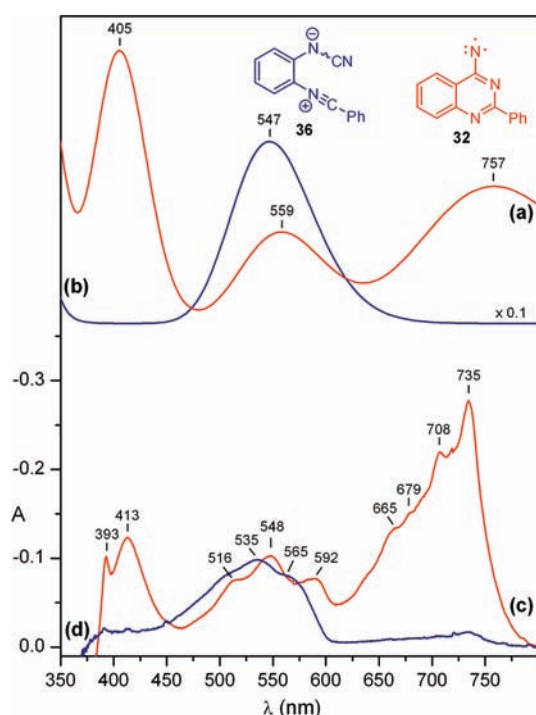


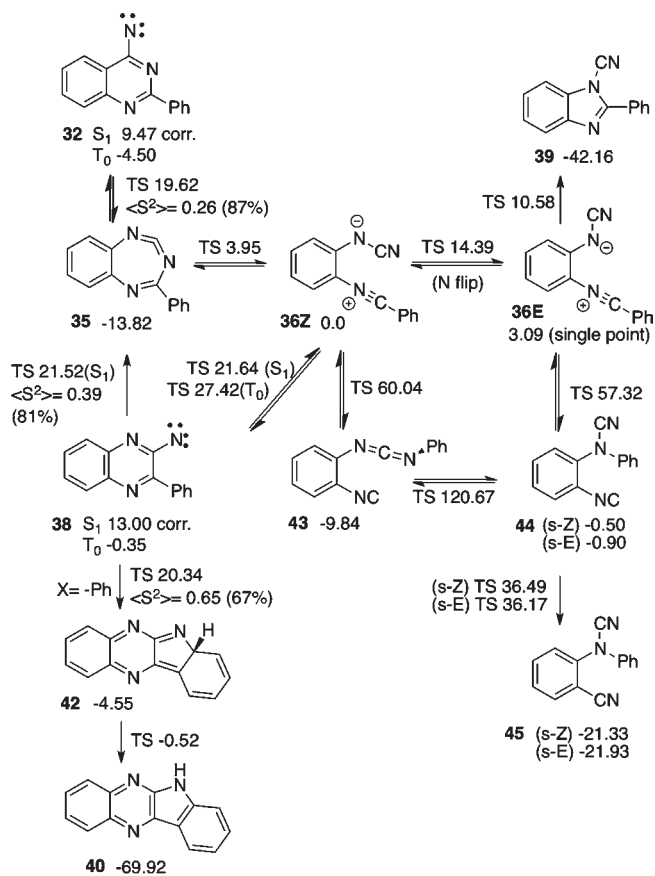
Figure 9. Observed and calculated UV–vis spectra of nitrene **32** and nitrile ylide **36**. Top: Calculated spectra; (a) red line: nitrene; (b) blue line: ylide (TD-B3LYP/6-31+G** convoluted using the SWizard program;¹¹ ordinate in arbitrary absorbance units). Bottom: Experimental difference spectra, inverted to show correlation with the calculated spectra. Positive peaks are disappearing on photolysis; red, nitrene; blue, ylide. Both are obtained in admixture by photolysis of azide **31A** at 308 nm for 23 min. (c) The nitrene is removed by photolysis at $\lambda > 610$ nm for 30 min (λ_{max} 735 and 548, and 413 nm). (d) The ylide is removed by photolysis at $\lambda > 395$ nm for 2 min (λ_{max} 535 nm). See also Figure S19 for further details.

(Figure 9) and the fact that the cyclic carbodiimide **35** was once again formed, as seen clearly in the IR difference spectrum of the same matrix (Figure S20). Accordingly, IR bands at 2281, 2141, and 2119 cm^{-1} can be assigned to the ylide **34** in good agreement with calculations (Figure S20). The ylide can exist in two conformers, **36Z** and **36E** (Scheme 8), which is presumably the reason for the double band at 2119 and 2141 cm^{-1} (Figure S19).

To summarize, the initial photolysis of the azide **31T** at 308 nm affords a mixture of nitrene **32**, the cyclic carbodiimide **35** and (little) ylide **36** (Figure S17) via the sequence azide \rightarrow nitrene \rightarrow cyclic carbodiimide \rightarrow ylide, because the nitrene absorbs slightly at 308 nm and undergoes further photoreaction. After bleaching the nitrene with visible light, the ylide becomes clearly observable in the UV–vis spectrum (Figure 9; its UV extinction coefficient is roughly 10 times higher than that of the nitrene). Its presence is obstructed in the initial IR spectrum due to the strong azide bands (see Figure S17). Intense spectra of the ylide were best formed by direct photolysis of the cyclic carbodiimide at 308 nm once the nitrene had been completely bleached at $\lambda > 610$ nm. Both the nitrene and the ylide form the cyclic carbodiimide on photolysis (Figures 10 and S20)

The cyclic carbodiimide **35** was also formed on matrix photolysis of tetrazoloquinoxaline **37T** at 308 nm, but this reaction was much less efficient, requiring several hours of

Scheme 8. Relative Energies of Ground and Transition State Structures (in kcal/mol) Calculated at the B3LYP/6-31G** Level



irradiation, because only a tiny amount of the azide **37A** was formed on mild FVT (250 °C), and the photolysis of the tetrazole was very slow.

Calculated energies of ground and transition state structures at the B3LYP/6-31G** level are summarized in Scheme 8. It is seen that the phenyl substitution has stabilized the ylide **36** significantly, so that it is now only ca. 14 kcal/mol higher in energy than the cyclic carbodiimide **35**. The barrier between them is small (18 kcal/mol from the carbodiimide side). The *s-E* ylide **36E** can cyclize via a very low barrier (ca. 8 kcal/mol) to the 1-cyanobenzimidazole **39**. Since the potential open-chain products **43**–**45** were not observed, the phenyl group is not seen to undergo 1,5- or 1,7-shifts. This is in accord with the much higher calculated barriers for the 1,5- and 1,7-shifts for phenyl (57 and 60 kcal/mol, respectively) than for H (9 and 13 kcal/mol, respectively; compare Schemes 5 and 8) or Cl (44 and 34 kcal/mol, respectively (vide supra)).

The triplet quinoxalinylnitrene **38T** may undergo ring opening to the triplet ylide **36** with a barrier of ca. 27 kcal/mol, but both singlet nitrenes **32** and **38** undergo ring expansion to the cyclic carbodiimide **35** very easily (ca. 9–10 kcal/mol). The cyclization of the singlet nitrene **38** to the 'isocarbazole'-type^{9,13} intermediate **42** (Scheme 8) also has a very low barrier (ca. 7 kcal/mol). The transition structures for the singlet nitrene reactions have 13–33% triplet contamination at

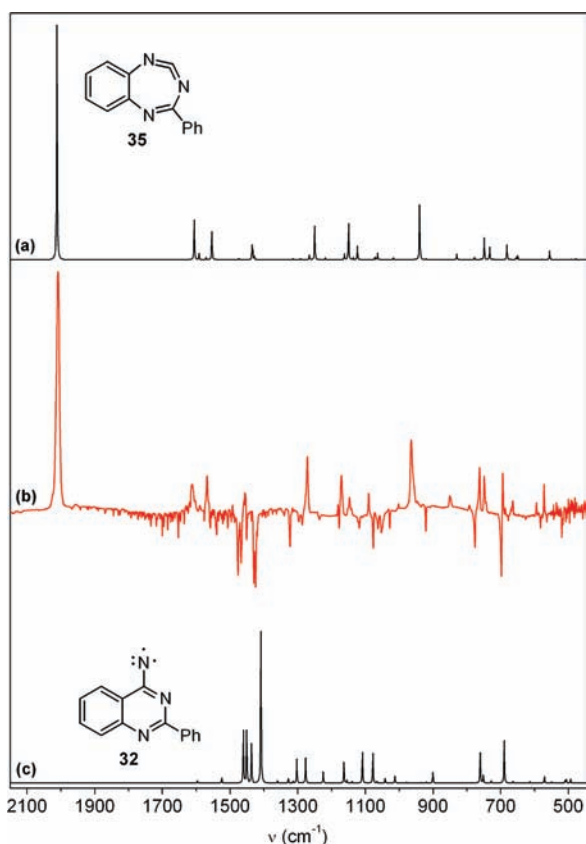


Figure 10. (a) Calculated IR spectrum of cyclic carbodiimide **35** (B3LYP/6-31G**). (b) IR difference spectrum from the photolysis of 4-azido-2-phenylquinazoline **31A** at 308 nm for 23 min (to generate nitrene **32**) followed by $\lambda > 610$ nm for 30 min (to destroy **32** and form **35** (2008 cm^{-1})). (c) Calculated IR spectrum of nitrene **32** (B3LYP/6-31G**). Ordinates in arbitrary absorbance units. See also Figure S20 for further details.

this computational level (data in Scheme 8; see discussion of errors in the context of Scheme 5).

Further strong evidence for the nitrene, the seven-membered ring, and the ylide was obtained in the 7-nitro-2-phenyl-4-quinazolinyl nitrene series (Scheme 9). Here, the extension of the conjugated system permitted selective photochemistry and clear-cut observation of all the interesting species.

Tetrazole **46T** was deposited through the FVT oven at $250\text{--}300\text{ }^{\circ}\text{C}$ to generate an Ar matrix of azide **46A**. Photolysis of this matrix at 308 nm generated the nitrene **47** (Scheme 9), which showed absorption maxima up to 754 nm in the UV-vis spectrum (Figure 11). Photolysis at $\lambda > 695$ nm converted the nitrene to the seven-membered ring carbodiimide **48** (UV λ_{max} 340 nm, Figure 11). The IR spectrum of the same matrix shows a characteristic strong absorption at 2014 cm^{-1} , and the spectrum is in excellent agreement with calculations (Figures 12 and S22). Further photolysis of this matrix at 308 nm caused ring opening of the carbodiimide **48** to the nitrile ylide **49** (UV-vis: Figure 13, λ_{max} 479–540 nm; IR: Figures 14 and S23). The *s-Z* and *s-E* conformers of the ylide, **49Z** and **49E**, have nearly identical IR spectra but slightly different UV-vis spectra, which allowed us to “separate” the two conformers spectroscopically (Figure S21). The *s-E* form was selectively destroyed at $\lambda > 550$ nm, and the *s-Z* form at $\lambda > 495$ nm (Figure S21), when they both cyclize back to

Scheme 9. 7-Nitro-2-phenyl-4-quinazolinyl nitrene: Relative Energies of Ground and Transition State Structures (in kcal/mol) Calculated at the B3LYP/6-31G** Level

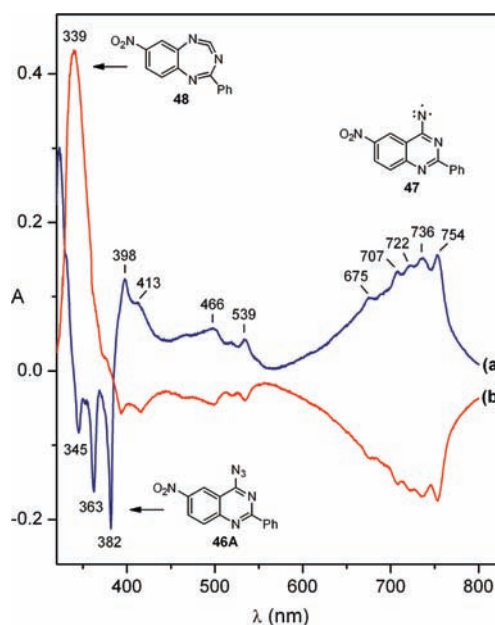
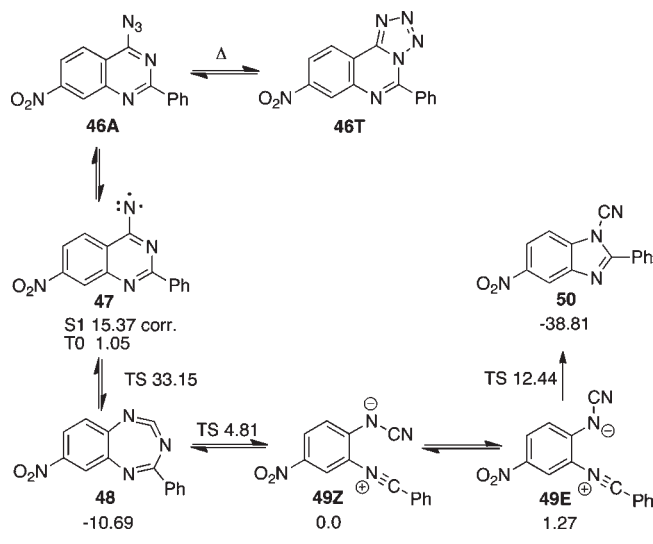


Figure 11. Blue line: UV-vis difference spectrum (Ar matrix, 10 K) showing formation of nitrene **47** (positive peaks) from azide **46A** (negative peaks) on irradiation of the azide at 308 nm for 2.5 min. Red line: UV-vis difference spectrum of nitrene **47** (negative peaks) and cyclic carbodiimide **48** (positive peak), formed on irradiation of the nitrene at $\lambda > 695$ nm for 9 h.

48. The UV-vis spectra are in excellent agreement with calculations at the TD-B3LYP/6-31+G** level (Figure S21). The complexity of the ylide absorptions near 2150 and 1300 cm^{-1} in the IR spectra may be due, at least in part, to the presence of the two conformers (Figures 14 and S23). Moreover, it was possible to cycle many times between the ylides and the seven-membered ring, as revealed by UV-vis (Figure 15) and IR spectroscopy (Figure 14), but eventually a small amount of the 1-cyanobenzimidazole **50** was also formed (2258 cm^{-1}). The

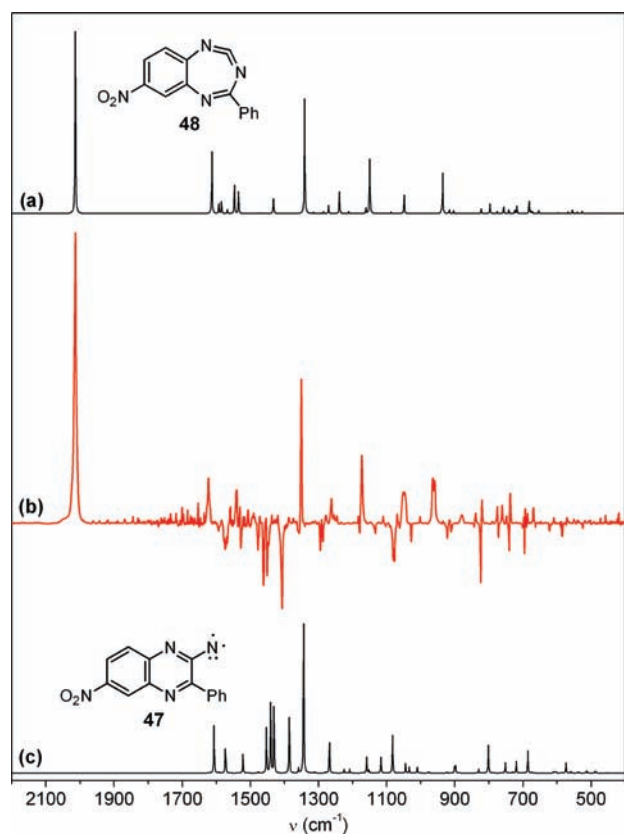


Figure 12. (a) Calculated IR spectrum of cyclic carbodiimide **48**. (b) Experimental difference spectrum showing disappearance of the nitrene **47** (negative peaks) and formation of the cyclic carbodiimide **48** on irradiation of the nitrene at $\lambda > 695$ nm for 9 h (same matrix as in Figure 11). (c) Calculated spectrum of nitrene **47**. All calculations at the B3LYP/6-31G** level.

same compound is formed in quantitative yield on FVT of **46** at 400–500 °C.

The calculated energies (Scheme 9) indicate that the difference between the nitrile ylide **49Z** and the cyclic carbodiimide **48** has now decreased further to ca. 11 kcal/mol. The activation barrier between the two is ca. 14 kcal/mol from the carbodiimide side and 5 kcal/mol from the ylide side. The barrier for cyclization of the ylide **49E** to 1-cyanobenzimidazole **50** is ca. 11 kcal/mol.

CONCLUSION

Tetrazoles **11T** and **13T** undergo valence tautomerisation to the corresponding azides **11A** and **13A** on mild flash vacuum thermolysis (FVT at ca. 250 °C). Photolyses of the tetrazole–azide mixtures in Ar matrixes at ca. 15 K afford the triplet nitrenes **12** and **14**, observed by ESR, UV, and IR spectroscopy. Matrix photolysis with IR observation demonstrates the rapid formation of the seven-membered ring carbodiimide **15** from both nitrenes, **12** and **14**. On further photolysis **15** disappears to be replaced by the open-chain carbodiimide **22**. The latter tautomerizes thermally to the cyanamide **23**.

The 5-methoxy- and 5-chlorotetrazolo[1,5-*a*]quinoxaline analogues **24a,b** afford the nitrenes **25a,b** and the ring-expanded carbodiimides **26a,b** cleanly on matrix photolysis. It is proposed

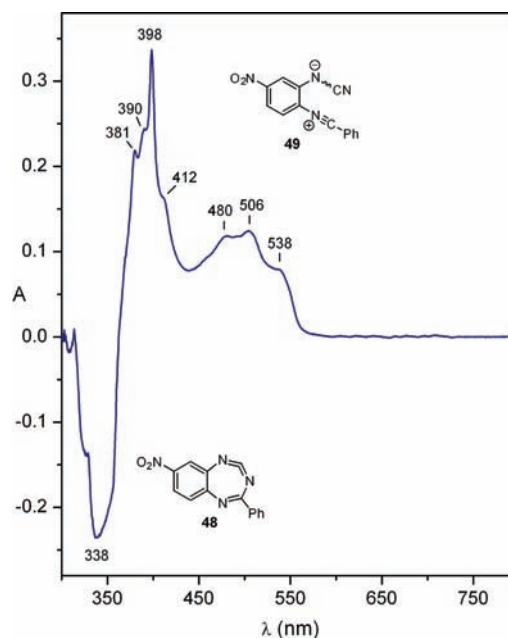


Figure 13. UV–vis difference spectrum of nitrile ylide **49** (positive peaks), obtained by irradiating the cyclic carbodiimide **48** (negative peak) at 308 nm for 50 min in Ar matrix at 10 K. **48** was obtained by prior photolysis of nitrene **47** (cf. Figures 11b and 12).

that the subsequent products (**16**, **17**, **22**, **23**, **28**) are formed via ring-opening of the seven-membered ring carbodiimides **15** and **26** and/or the 2-quinoxalinylnitrenes **12** and **25** to the nitrile ylides **21** and **27**, respectively (Schemes 4–7).

5-Phenyltetrazolo[1,5-*a*]quinazoline/4-azido-2-phenylquinazoline **31T/31A** and the corresponding quinoxaline **37T/37A** give rise to the two nitrenes **32** and **38** as well as the seven-membered ring carbodiimide **35** and the nitrile ylide **36**, which were characterized by UV and IR spectroscopy. In the similar case of 7-nitro-5-phenyltetrazolo[1,5-*a*]quinazoline, nitrene **47**, cyclic carbodiimide **48**, and nitrile ylide **49** are identified by UV and IR spectroscopy, and **48** and **49** undergo reversible photochemical interconversion.

The extended conjugated systems in the phenyl-substituted series caused a wider spread of absorption maxima, thus, permitting selective photochemistry and characterization of nitrenes, cyclic carbodiimides, and nitrile ylides. Moreover, the phenyl groups cause the calculated energy difference between the cyclic carbodiimides and the nitrile ylides to decrease to 11–14 kcal/mol, and the barrier toward further rearrangements of the ylides to increase (1,5- and 1,7-shifts to open-chain cyanamides and carbodiimides, and ring closure to 1-cyanobenzimidazoles).

Recyclization of open-chain nitrile ylides emerges as an important mechanism of formation of ring-contraction products. Thus, ring expansion and ring contraction become consecutive processes according to the sequence hetarylnitrene → cyclic carbodiimide → open-chain nitrile ylide → cyanobenzimidazole. This generalized sequence can be expected to apply to many other hetarylnitrenes.

EXPERIMENTAL SECTION

General procedures for Ar matrix isolation with IR spectroscopy at 10 K^{3,4,14} and ESR spectroscopy at 15 K,⁶ and flash vacuum thermolysis (FVT)¹⁵ have been published. A 1000 W high pressure Hg/Xe lamp

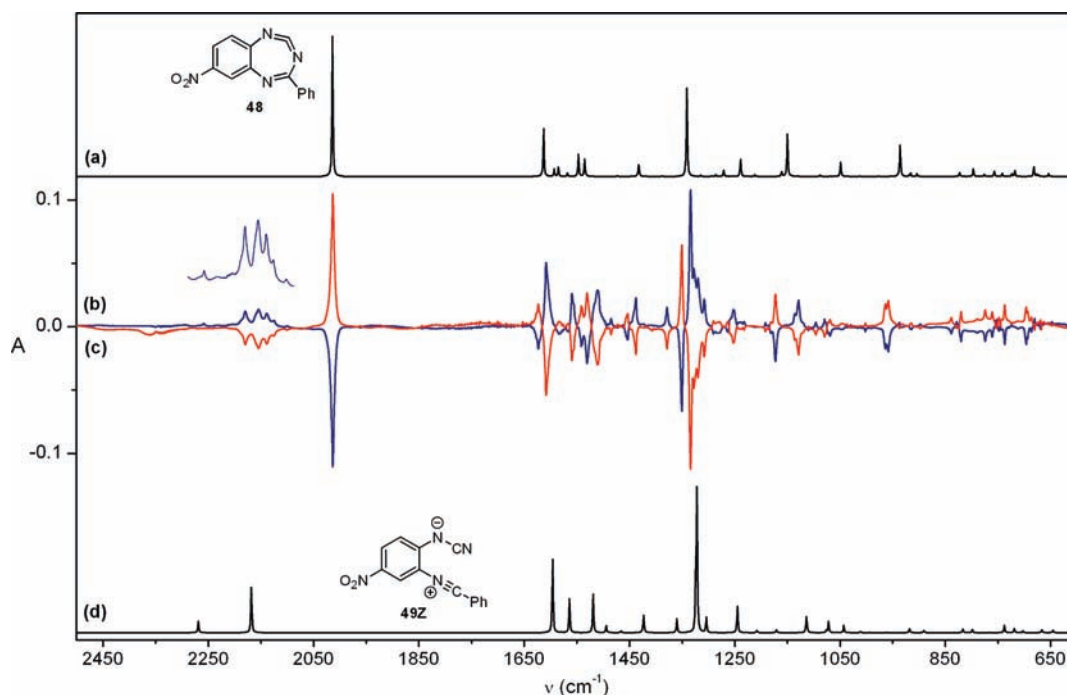


Figure 14. (a) Calculated IR spectrum of carbodiimide **48**. (b and c) Interconversion of cyclic carbodiimide **48** (positive, blue spectrum; negative, red spectrum) and nitrile ylide **49** (positive, red spectrum; negative, blue spectrum) in Ar matrix at 10 K. Irradiation of the carbodiimide at 308 nm for 20 min gives the ylide **49**. Irradiation of the ylide at $\lambda > 495$ nm for 25 min gives the carbodiimide **48**. It was possible to cycle several times between these two spectra. (d) Calculated IR spectrum of nitrile ylide **49**. All calculations at the B3LYP/6-31G** level.

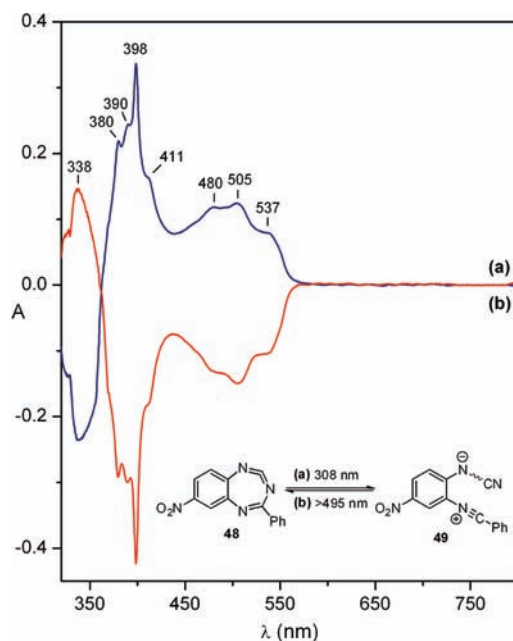


Figure 15. UV-vis difference spectra (Ar matrix, 10 K) showing reversible interconversion of nitrile ylide **49** and cyclic carbodiimide **48** on irradiation at $\lambda = 308$ nm for 20 min (forming ylide **49**) and at $\lambda > 495$ nm for 25 min (forming carbodiimide **48**). It was possible to cycle several times between these two spectra.

with appropriate filters, 75 W low pressure Hg lamps, or excimer lamps operating at 222 nm (25 mW/cm^2) and 308 nm (50 mW/cm^2) were used for irradiation. Details of preparation and matrix isolation are given in the Supporting Information.

■ ASSOCIATED CONTENT

S Supporting Information. Additional ESR, IR, UV, and NMR spectra, a GC-MS, Figures S1–S26, further experimental details, computational methods, Cartesian coordinates, vibrational frequencies and energies of all calculated molecules and transition structures at the (U)B3LYP/6-31+G** level. This material is available free of charge via the Internet at <http://pubs.acs.org>.

■ AUTHOR INFORMATION

Corresponding Author
wentrup@uq.edu.au

■ ACKNOWLEDGMENT

This work was supported by the Australian Research Council. We are indebted to the APAC National Facility and the Centre for Computational Molecular Science at the University of Queensland for generous access to supercomputing, to Dr. Chris Noble (Centre for Magnetic Resonance, The University of Queensland) for performing simulations of ESR spectra, to Dr. Chris Addicott for preliminary experiments on **31T** and **37T**, and to Ms. Sieglinde Ebner from the Universität Graz, Austria, for preliminary experiments on **24Ta** and **26a**.

■ REFERENCES

- (1) Bednarek, P.; Wentrup, C. *J. Am. Chem. Soc.* **2003**, *125*, 9083.
- (2) (a) Chapman, O. L.; LeRoux, J.-P. *J. Am. Chem. Soc.* **1978**, *100*, 282. (b) Hayes, J. C.; Sheridan, R. S. *J. Am. Chem. Soc.* **1990**, *112*, 5879. (c) Kuhn, A.; Vosswinkel, M.; Wentrup, C. *J. Org. Chem.* **2002**,

67, 9023. (d) Maltsev, A.; Bally, T.; Tsao, K.-L.; Platz, M. S.; Kuhn, A.; Vosswinkel, M.; Wentrup, C. *J. Am. Chem. Soc.* **2004**, *126*, 237.

(3) Kvaskoff, D.; Mitschke, U.; Addicott, C.; Finnerty, J.; Bednarek, P.; Wentrup, C. *Aust. J. Chem.* **2009**, *62*, 275.

(4) Addicott, C.; Wong, M. W.; Wentrup, C. *J. Org. Chem.* **2002**, *67*, 8538.

(5) Griffin, M.; Muys, A.; Noble, C.; Wang, D.; Eldershaw, C.; Gates, K.; Burrage, K.; Hanson, G. *Mol. Phys. Rep.* **1999**, *60*.

(6) Kvaskoff, D.; Bednarek, P.; George, L.; Waich, K.; Wentrup, C. *J. Org. Chem.* **2006**, *71*, 4049.

(7) Wentrup, C. *Tetrahedron* **1971**, *27*, 367.

(8) Johnson, W. T. G.; Sullivan, M. B.; Cramer, C. J. *Int. J. Quantum Chem.* **2001**, *85*, 492.

(9) Tsao, M.-L.; Gritsan, N. P.; James, M. S.; Platz, M. S.; Hrovat, D. A.; Borden, W. T. *J. Am. Chem. Soc.* **2003**, *125*, 9343.

(10) Kvaskoff, D.; Bednarek, P.; Wentrup, C. *J. Org. Chem.* **2010**, *75*, 1600.

(11) Gorelsky, S. I. *SWizard program*; University of Ottawa: Ottawa, Canada, 2010; <http://www.sg-chem.net/> (accessed November 2010).
Gorelsky, S. I.; Lever, A. B. P. *J. Organomet. Chem.* **2001**, *635*, 187.

(12) Wentrup, C.; Thétaz, C.; Tagliaferri, E.; Lindner, H. J.; Kitschke, B.; Winter, H.-W.; Reisenauer, H. P. *Angew. Chem., Int. Ed. Engl.* **1980**, *19*, 566. Wentrup, C. *Top. Curr. Chem.* **1976**, *62*, 175.
Wentrup, C.; Thétaz, C.; Gleiter, R. *Helv. Chim. Acta* **1972**, *55*, 2633.

(13) Wentrup, C. *Adv. Heterocycl. Chem.* **1981**, *28*, 231.

(14) Kuhn, A.; Plüg, C.; Wentrup, C. *J. Am. Chem. Soc.* **2000**, *122*, 1945. Kappe, C. O.; Wong, M. W.; Wentrup, C. *J. Org. Chem.* **1995**, *60*, 1686.

(15) Wentrup, C.; Blanch, R.; Briehl, H.; Gross, G. *J. Am. Chem. Soc.* **1988**, *110*, 1874.